J Therm Anal Calorim (2011) 104:627–633
DOI 10.1007/s10973-010-1099-8

DSC study of the kinetic parameters of the metastable phases formation during non-isothermal annealing of an Al–Si–Mg alloy

Mourad Ibrahim Daoudi · Abdelhafid Triki · Abdelkrim Redjaimia

Received: 28 June 2010 / Accepted: 6 October 2010 / Published online: 26 October 2010

Abstract Kinetics of β'' and β' precipitations in an AlSiMg have been studied under non-isothermal conditions using differential scanning calorimetry (DSC) technique. The variation of the activation energy as a function of transformed fraction is determined using two isoconversional methods of Kissinger–Akahira–Sunose (KAS) and Friedman. The results obtained using the two methods show a change in the activation energy for both metastable phases precipitations as a function of transformed fraction. The results obtained from KAS method as compared with those obtained from Friedman method, show some major disagreements between the two methods. The growth exponent, determined by Ozawa method, decreases as a function of temperature for both phases.

Keywords Al–Si–Mg alloy · DSC · Kinetic parameters · Isoconversional methods

Introduction

Solid-state phase transformations lead to an important change in microstructure and hence in mechanical properties of alloys. It is important, then, to understand the process of phase transformation in order to optimize the microstructure.

Phase transformations occur during both isothermal and non-isothermal annealing, involving several nucleation and growth mechanisms as summarized by Kempen et al. [1], for example. The most important kinetic parameters for solid-state phase transformation are the activation energy (Q_α), and the growth exponent (n). The determination of these two parameters and their evolution with respect to time and temperature is of great importance to understand the phase transformation mechanisms.

The kinetics of solid-state reaction performed under non-isothermal conditions at linear heating rate $\phi = \mathrm{d}T/\mathrm{d}t$, can be described by the following rate equation [2–4]:

$$\frac{\mathrm{d}\alpha}{\mathrm{d}T} = \frac{A}{\phi}\mathrm{e}^{-Q/RT} \cdot f(\alpha) \tag{1}$$

where $f(\alpha)$ is a function of the transformed fraction, α, that depends on the reaction model, Q_α is the activation energy. There are many methods for determining the activation energy from experiments under non-isothermal condition and a linear heating rate. Isoconversional methods, which permit activation energy to be determined as a function of the transformed fraction, are the most generally used.

The differential isoconversional methods suggested by Friedman [5] is based on the Eq. 2

$$\mathrm{Ln}\left(\phi\frac{\mathrm{d}\alpha}{\mathrm{d}T}\right)_\alpha = \mathrm{Const} - \frac{Q_\alpha}{RT} \tag{2}$$

For various heating rates ϕ_i, the activation energy Q_α, for a given transformed fraction α, is estimated from the plot of Ln $(\phi\ \mathrm{d}\alpha/\mathrm{d}T)_{\alpha i}$ versus $1/RT_{\alpha i}$.

The integral isoconversional methods are based on the integral form of Eq. 1

M. I. Daoudi (✉)
Physics Department, University of Guelma Algeria and LM2S Laboratory, Annaba, Algeria
e-mail: mdaoudi@voila.fr

A. Triki
Physics Department, University of Annaba and LM2S Laboratory, Annaba, Algeria

A. Redjaimia
Institut Jean Lamour, Ecole des Mines de Nancy, Parc de Saurupt, CS 14 234, 54042 Nancy cedex, France

$$g(\alpha,0)=\int_0^{\alpha}\frac{\mathrm{d}\alpha}{f(\alpha)}=\frac{A}{\phi}\int_0^{T}\mathrm{e}^{-Q/RT}\mathrm{d}T=\frac{AQ}{\phi R}p(x) \quad (3)$$

where $x = Q/RT$. Using the more precise approximation by Coats and Redfern [6] for $p(x)$, we get the Kissinger–Akahira–Sunose (KAS) [7, 8] method based on Eq. 4:

$$\mathrm{Ln}\left(\frac{\phi_i}{T_{\alpha_i}^2}\right)=\mathrm{const}-\frac{Q_\alpha}{RT_{\alpha i}} \quad (4)$$

For a given transformed fraction α, Q_α can be estimated from a plot of $\mathrm{Ln}\left(\phi_i/T_{\alpha_i}^2\right)$ versus $1/RT_{\alpha i}$. Similar equation has been proposed by Mittemeijer [9].

Others methods have been proposed that can deal with variable activation energies. These methods include, in addition to the method of Friedman, the advanced nonlinear isoconversional method developed by Vyazovkin [10], a new iterative linear isoconversional method by Cai and Chen [11], the method of Ortega [12],…etc.

Phase transformation in Al–Si–Mg metallic alloys occurs via the generally accepted precipitation sequence [13–16]:

$$\mathrm{SSS}\rightarrow\text{Solute Clusters}\rightarrow\mathrm{GPZ}\rightarrow\beta''\rightarrow\beta'\rightarrow\beta$$

where SSS represents the super-saturated solid solution, GPZ stands for Guinier–Preston zones, β'' are metastable needle-like precipitates, β' are metastable rod-like (or lath-like) precipitates and β is the equilibrium phase. β'' and β' precipitations occur by nucleation and growth and are diffusion controlled-growth.

Most of the studies on β'' and β' phases in AlSiMg alloys have been particularly focused on the qualitatively complex precipitation sequence [17–19] and crystal structures [15, 20–22].

The present work has been undertaken to investigate the evolution of the kinetic parameters associated to the metastable phases formation, during non-isothermal annealing of an AlSiMg alloy at different constant heating rates. The differential scanning calorimetry (DSC) data is analyzed with the help of the isoconversional methods of Kissinger–Akahira–Sunose (KAS) and Friedman. These isoconversional methods are extensively used for analysing non-isothermal decomposition, crystallization and degradation kinetics for large variety of materials and compounds such, polymers [23–25], glasses [26, 27], liquid crystals [28] and others [29, 30].

Experimental

The tested Al–Si–Mg alloy was received in an extruded state and has the chemical composition (wt%) given in Table 1:

Table 1 Alloy composition (wt%)

Si	Mg	Mn	Fe	Cr	Cu	Al
1.195	0.587	0.480	0.231	0.112	0.030	97.365

The excess Si with respect to the balanced Al–Si–Mg alloy is calculated using the relation reported by Gupta et al. [18] in which we have added the Mn effect whose role is similar to the Fe one [31] (Eq. 5).

$$\text{Excess Si}=(\text{wt\% in alloy})-\left[\left(\frac{\text{wt\%Mg in alloy}}{1.73}\right)\right]-\left[\left(\frac{\text{wt\% Fe in alloy}}{4}\right)+\left(\frac{\text{wt\% Mn in alloy}}{4}\right)\right] \quad (5)$$

The alloy was solutionized at 540 °C for 1 h, and subsequently water quenched. The tested samples were machined from the homogenized alloy. They have been cut in a disc form of 5 mm of diameter and 3 mm of height, having an average weight of 225 mg. Differential scanning calorimetry (DSC) analysis of the samples was performed in a purified argon atmosphere, using a SETARAM 131 instrument. Aluminium crucibles are used. High purity aluminium (99.999) was used as a reference material. Temperature scans were made from 20 to 600 °C with constant heating rates of 5, 10, 15, 20 and 30 K/min.

Transmission electronic microscopy (TEM) experiments were performed with a conventional Philips CM-12 operated at 120 kV. Specimens were thinned in Tenupol-2 jet-polisher for which the electrolyte was kept below room temperature and a potential of 12 V. The electrolyte was composed of perchloric acid (18%), glycerol (18%) and ethanol (64%).

Results and discussion

DSC experiments

The precipitation sequence for the alloy under study has been determined by performing the DSC scan shown in Fig. 1a, obtained at heating rate of $\phi = 10$ K/min for a sample solutioned and subsequently water quenched. As corroborated by previous publications [15, 17, 20–22], the exothermic peaks are related to the formation of GPZ, β'', β' and β phases, formation, respectively, at around 100, 250, 300 and 500 °C.

Differential scanning calorimetry (DSC) scans obtained in the same way at different heating rates of $\phi = 5$, 10, 15, 20 and 30 K/min are shown in Fig. 1b. Exothermic reaction peaks are shifted towards higher temperatures as

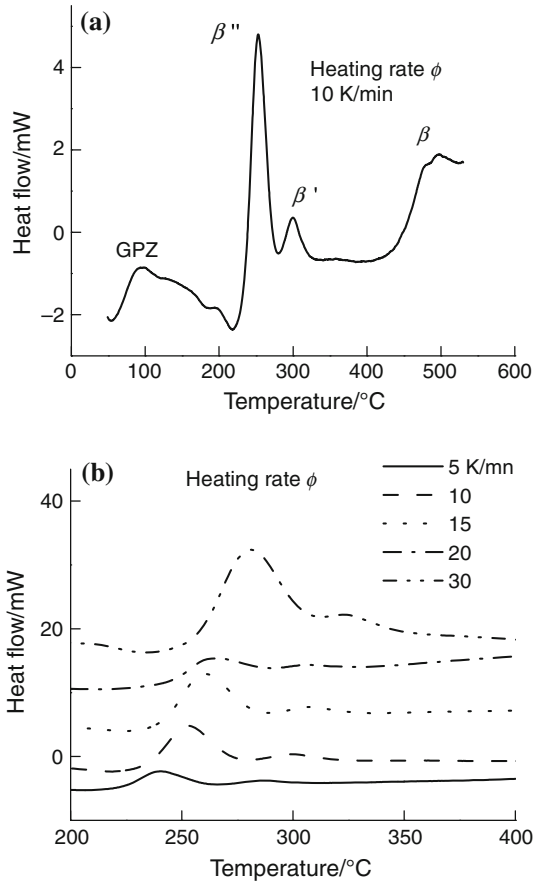

Fig. 1 DSC scans for Al–Si-Mg alloy under study obtained at heating rates of: (**a**) $\phi = 10$ K/min. (**b**) $\phi = 5$, 10, 15, 20 and 30 K/min

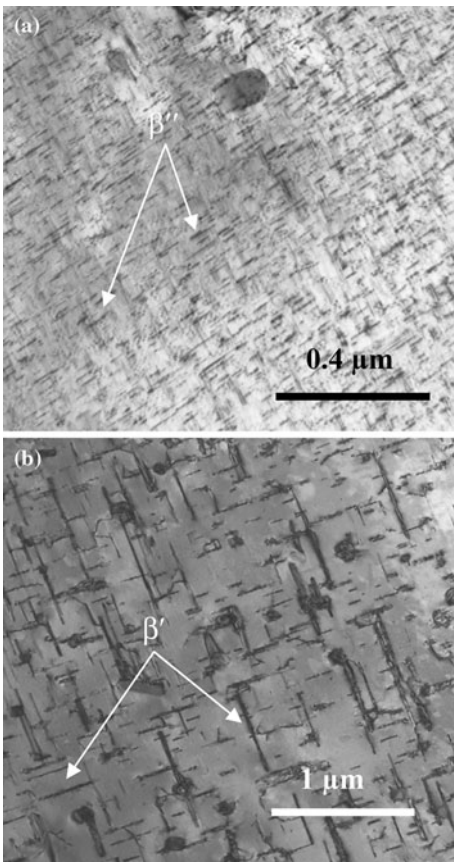

Fig. 2 Bright field TEM micrographs showing: (**a**) Needle-like β'' precipitates and (**b**) rod-like β' precipitates

function of heating rates, which means that these transformations are thermally activated.

In order to display β'' and β' precipitates, two samples are heated at 10 K/min up to 240 °C for the first and up to 300 °C for the second, both aged for 5 min and 1 h, respectively, and then water quenched. It is expected to obtain the β'' and β' precipitations, respectively, for the two treatment procedures.

Indeed, Fig. 2 shows needle-like β'' and rod-like β' precipitates as indicated by arrows in the micrographs.

Non-isothermal transformation

The transformed fraction α, as a function of temperature for different heating rates is shown in Fig. 3, for both β'' and β' transformations, is obtained from the DSC curves by integrating the surface area under the exothermic peaks. Increasing the heating rates pushes up the onset temperature for the transformation. Moreover, at fixed temperature, the transformation is promoted by using lower heating rates.

Determination of the activation energy

In order to investigate the variation of the activation energy with extent of conversion, KAS and Friedman isoconversional methods are used, and the activation energy values are determined using Eq. 4 for KAS method and Eq. 2 for Friedman method, by choosing a number of α values. Figures 4 and 5 display the dependence of Q_α on the transformed fraction α, respectively, for the two methods. As shown in these figures, the variation of the activation energy as a function of the transformed fraction, α, is observed for the two methods. For the KAS method, the average value of the activation energy associated with the β'' precipitation, decreases gradually with increasing transformed fraction from about 105 to 92 kJ/mol. In contrast, the average value of the activation energy associated with β' precipitation increases with increasing transformed fraction from about 132 to 141 kJ/mol. These values are close to the reported values of diffusion of Mg, Si and Al in aluminium matrix which are in the range from 124 to 142 kJ/mol [32–36]. For Friedman method, the average value of the activation energy associated with β'' precipitation, increases gradually then becomes practically

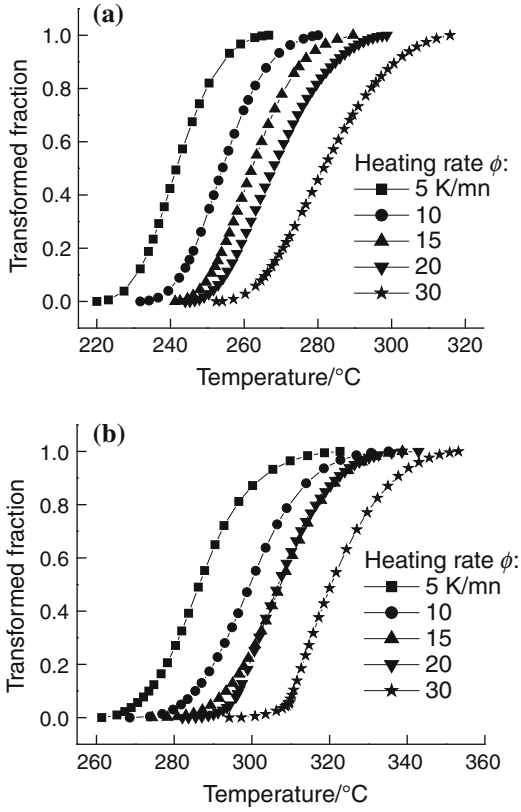

Fig. 3 Evolution of the transformed fraction α, as a function of temperature for different heating rates. (**a**) for β'' and (**b**) for β' transformations

constant for transformed fraction $\alpha > 0.5$, at a value of 26 kJ/mol (Fig. 5a). The average value of the activation energy associated with β' precipitation, increases also gradually, reaches a maximum at value of 84 kJ/mol, then decreases to a value of 61 kJ/mol corresponding to a transformed fraction value of 0.9 (Fig. 5b).

The comparison between the results obtained from the two methods shows two major disagreements. The first concerns the tendency of the activation energy variation for β'' precipitation. Figures 4a and 5a show that the application of KAS method lead to a decrease of Q_α as a function of α, whereas in the case of Friedman method, the activation energy increases with increasing α. The second one is that the values of the activation energy determined by Friedman method are much smaller than the values determined by the other method. The latter disagreement has been reported for non-isothermal crystallization of amorphous alloys [37, 38]. As pointed out by Vyazovkin [10], Starink [39] and Ortega [12], the Friedman method tends to be numerically unstable, especially when the rate $d\alpha/dT$ is estimated by numerical differentiation of experimental data, which is the case in this work. This could lead to smaller values for Q_α

The change in the activation energy as a function of transformed α, observed in the study of β'' and β' non-isothermal precipitations, could be an indication for multi-step reactions involving different mechanisms operating at

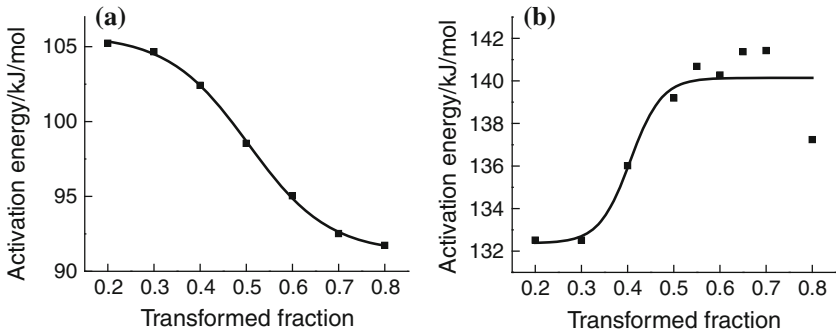

Fig. 4 Evolution of the activation energy Q_α as a function of the degree of transformed fraction α. KAS method. (**a**) for β'' and (**b**) for β' transformations

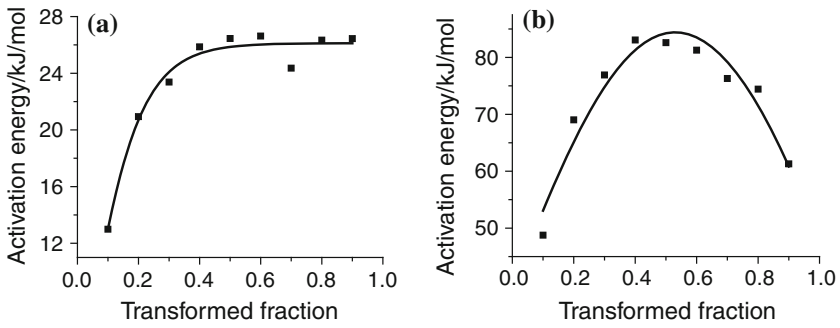

Fig. 5 Evolution of the activation energy Q_α as a function of the degree of transformed fraction α. Friedman method. (**a**) for β'' and (**b**) for β' transformations

different degree of transformation, having likely different activation energies.

The analysis of the variation of the activation energy in order to understand the physical mechanisms related to this change is not evident. However, this behaviour can be tentatively explained, for KAS results, as follows.

Nucleation of β'' precipitates takes place on to pre-existing precipitates constituting a phase called pre-β'' reported by Marioara et al. [40] in alloys having excess Si, which is estimated to be 0.68 for the alloy under study, using Eq. 5. Gupta et al. [18] and Murayama and Hono [41] show that the excess Si promotes the formation of a larger amount of (Mg + Si) clusters and GPZ. Pre-β'' phase, which is the more developed GPZ, is fully coherent with the matrix. It contains Mg, Si and a substantial amount of Al. The transformation of pre-β'' to β'' involves a continuous replacement of Al atoms with Mg and in a less extent by Si atoms released from clusters and the solid solution [40–44]. As more Mg and Si are added to the pre-β'' precipitates, the ratio Mg/Si tends to the stoichiometry of the β'' phase (Mg_5Si_6). It is obvious that both quenched-in vacancies and solute-vacancy complexes formation, play a direct role in the pre-$\beta'' \rightarrow \beta''$ structural transition. The high bounding energy of solute-vacancy complexes tends to stabilize the pre-β'' phase during early stages of the transformation, because of the lower mobility of bound vacancies. However, its efficiency gradually decreases during continuous heating, which can explain the Q_α decrease.

Figure 4 shows also that the Q_α average value is practically constant for lower transformed fraction, increases somewhat rapidly and becomes again constant for higher transformed fraction. Nevertheless it tends to decrease for latter stages of growth. Starink and Zahra [45] and Kempen et al. [1] suggest that the Q_α of the transformation can be interpreted as a combination of the constant activation energy for nucleation (Q_N) and growth (Q_G). According to this suggestion, the average value corresponding to the first plateau could be attributed to Q_N and the average value corresponding to the second value at higher transformed fraction to Q_G. Then, during the course of the transformation, the Q_α is likely predominating nucleation type and tends gradually towards predominating growth type.

Growth exponent $n(T)$

The values of n as a function of temperature, T, can be determined using Eq. 6 [46, 47].

$$\frac{d[\mathrm{Ln}(-\mathrm{Ln}(1-\alpha_T))]}{d\mathrm{Ln}\phi} = n(T)_\phi \quad (6)$$

where, α_T represents the transformed fraction attained at a certain fixed value of T, as measured for different heating rates. The dependence of n (at fixed ϕ) on T, $n(T)_\phi$, can be determined by choosing different T values. Variation of n with respect to temperature are presented in Fig. 6, for the β'' and β' transformations, respectively.

As shown in Fig. 6, n is temperature dependent and decreases for both phases, from the value $n = 4$ to about 2.3 for β'' and from the value $n = 4$ to about 1 for β' transformations, respectively.

As predicted by the classic theory [48] for the nucleation and diffusion-controlled growth, the n values depend on nucleation rate and the dimensionality growth and are in the range of 1 to 2.5, except for the increasing nucleation rate case where the n is superior to 2.5. The value $n = 4$ determined in the present study, seems to be overestimated, but remains superior to 2.5. It can be associated with an increased nucleation rate. One suggests that during continuous heating, more and more particles dissolve and the Mg and Si atoms released diffuse easily towards other pre-β'' precipitates which transform into β'' particles.

Growth exponent for β' transformation tends to the value $n = 1$. It agrees with the one predicted for the thickening of large rod-like precipitates [49]. β' precipitates are effectively rod-like. By another way, Tsao et al.

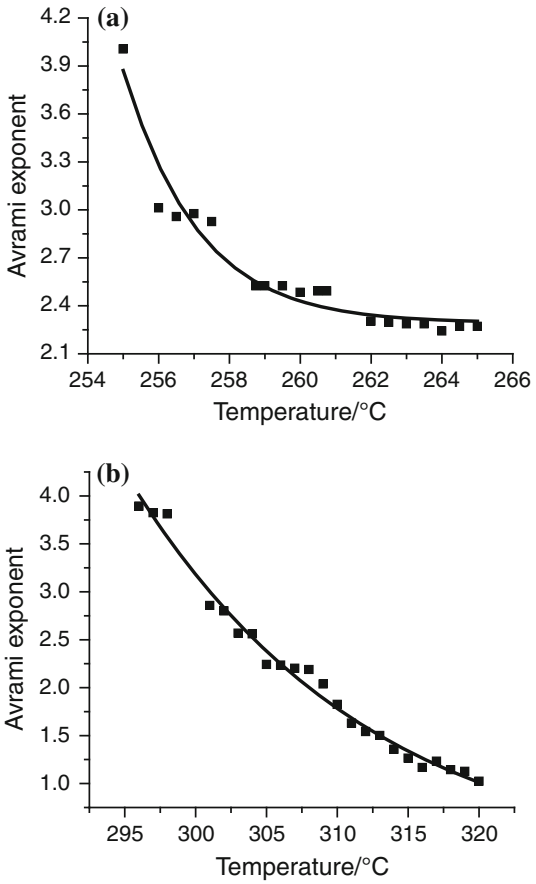

Fig. 6 Variation of the growth exponent as a function of temperature T for: (**a**) β'' transformation. (**b**) β' transformation

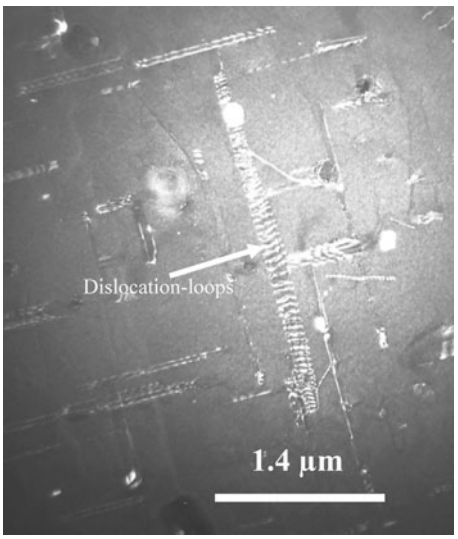

Fig. 7 TEM weak beam dark field micrograph. Interface β'/matrix dislocation-loops

[31], using in situ synchrotron small-angle X-ray scattering (SAXS) analysis, have investigated the evolution of β'' and β' precipitates in an AA6022 AlSiMg alloy.

They show that the radius of rod-like β' precipitates increases obviously during the growth stage, in contrast for β'' radius that remains practically constant. The thickening of the rod-like β' precipitates could be related to the formation of dislocation-loops surrounding the precipitates (Fig. 7). The dislocation-loops have been observed in similar alloys, by Weatherly and Nicholson [49] and Jacobs [20], and are related to the loss of coherency between precipitates and matrix during the last stage of growth. The presence of those dislocation loops, surrounding β' precipitates, more likely promotes their thickening.

Conclusions

The evolutions of the kinetic parameters, activation energy, Q_α and growth exponent, n, corresponding to the β'' and β' precipitations under non-isothermal conditions have been studied using DSC experiments.

The variation of the activation energy as a function of transformed fraction is obtained by means of KAS and Friedman isoconversional methods.

The variation of the growth exponent is obtained using Ozawa method.

The following conclusions can be drawn:

- The activation energy determined from the two methods was found to vary with the transformed fraction for both β'' and β' precipitations.
- The results obtained from KAS method as compared with those obtained by Friedman method show two major disagreements between the two methods:
  - Friedman method leads to a much smaller values of the activation energy.
  - For β'' precipitation, the activation energy was found to decrease as a function of the transformed fraction, for KAS method and to increase in the case of Friedman method.
- The exponent growth decreases as a function of temperature for both β'' and β' precipitations.

References

1. Kempen ATW, Sommer F, Mittemeijer EJ. Determination and interpretation of isothermal and non-isothermal transformation kinetics; the effective activation energies in terms of nucleation and growth. J Mater Sci. 2002;37:1321–32.
2. Brown ME, Dollimore D, Galwey AK. Comprehensive chemical kinetics. In: Bamford H, Tipper CFH, editors. Reaction in the solid state, vol. 22. Amsterdam: Elsevier; 1980. p. 41–113.
3. Šesták J. Thermophysical properties of solids, their measurements and theoretical thermal analysis. Amsterdam: Elsevier; 1984.
4. Galwey AK, Brown ME. Thermal decomposition of ionic solids. Amsterdam: Elsevier; 1999.
5. Friedman HL. Kinetics of thermal degradation of char-forming plastics from thermogravimetry. Application to a phenolic plastic. J Polym Sci C. 1964;6:183–95.
6. Coats AW, Redfern JP. Kinetic parameters from thermogravimetric data. Nature. 1964;201:68–9.
7. Kissinger HE. Reaction kinetics in differential thermal analysis. Anal Chem. 1957;29:1702–6.
8. Akahira T, Sunose T. Trans. Joint Convention of Four Electrical Institutes, Paper No. 246, 1969 Research report. Chiba Institute of Technology. Sci Technol. 1971;16:22–31.
9. Mittemeijer EJ. Analysis of the kinetics of phase transformations. J Mater Sci. 1992;27:3977–87.
10. Vyazovkin S. Modification of the integral isoconversional method to account for variation in the activation energy. J Comput Chem. 2001;22:178–83.
11. Cai J, Chen S. A new iterative linear integral isoconversional method for the determination of the activation energy varying with the conversion degree. J Comput Chem. 2009;30:1986–91.
12. Ortega A. A simple and precise linear integral method for isoconversional data. Thermochim Acta. 2008;474:81–6.
13. Wahi RP, von Heimendahl M. On the occurence oft he metastable phase β'' in Al–Si–Mg alloy. Phys Stat Sol A. 1974;24:607–12.
14. Burger GB, Gupta AK, Jeffrey PW, Lloyd DJ. Microstructural control of aluminum sheet used on automotive application. Mater Charact. 1995;35:23–39.
15. Andersen SJ, Zandbergen HW, Jansen J, Træholt C, Tundal U, Reiso O. The crystal structure of the β'' phase in Al–Mg–Si alloys. Acta Mater. 1998;46:3283.
16. Miao WF, Laughlin DE. Precipitation hardening in aluminum alloy 6022. Scripta Mater. 1999;40:873–8.
17. Dutta I, Allen SM. A calorimetric study of precipitation in commercial aluminium alloy 6061. J Mater Sci Lett. 1991;10:323–6.

18. Gupta AK, Lloyd DJ, Court SA. Precipitation hardening in Al–Mg–Si alloys with and without excess Si. Mater Sci Eng A. 2001;316:11–7.
19. Wang X, Esmaeili S, Lloyd DJ. The sequence of precipitation in the Al–Mg–Si–Cu alloy AA6111. Metall Mater Trans A. 2006;37A:2691–9.
20. Jacobs MH. The structure of the metastable precipitates formed during ageing of an Al–Mg–SI alloy. Philos Mag. 1972;26:1–13.
21. Edwards GA, Stiller K, Dunlop GL, Couper MJ. The precipitation sequence in Al–Mg–Si alloys. Acta Mater. 1998;46:3893–904.
22. Matsuda K, Naoi T, Fujii K, Uetani Y, Sato T, Kamio A, Ikeno S. Crystal structure of the β'' phase in an Al-1.0mass%Mg_2Si-0.4mass%Si alloy. Mater Sci Eng A. 1999;262:232–7.
23. Polli H, Pontes LAM, Araujo AS, Barros Joana MF, Fernandes VJ Jr. Degradation behavior and kinetic study of ABS polymer. J Therm Anal Calorim. 2009;95:131–4.
24. Chrissafis K. Kinetics of thermal degradation of polymers. Complementary use of isoconversional and model-fitting methods. J Therm Anal Calorim. 2009;95:273–83.
25. Kumari K, Raina KK, Kundu PP. DSC studies on the curing of chitosan-alanine using glutaraldehyde as crosslinker. J Therm Anal Calorim. 2009;98:469–76.
26. Păcurariu C, Lazău RI, Lazău I, Ianos R, Tita B. Non-isothermal crystallization kinetics of some basaltic glass-ceramics containing CaF_2 as nucleation agent. J Therm Anal Calorim. 2009;97:507–13.
27. Araújo EB, Idalgo E. Studies on crystallization kinetics of tellurite $20Li_2O$–$80TeO_2$ glass. J Therm Anal Calorim. 2009;95:37–42.
28. Rotaru A, Moantă A, Rotaru P, Segal E. Thermal decomposition kinetics of some aromatic azomonoethers. Part III. Non-isothermal study of 4-[(4-chlorobenzyl)oxy]-4′-chloroazobenzene in dynamic air atmosphere. J Therm Anal Calorim. 2009;95:161–6.
29. López M, Blanco M, Vazquez A, Ramos JA, Arbelaiz A, Gabilondo N, Echeverría JM, Mondragon I. Isoconversional kinetic analysis of resol-clay nanocomposites. J Therm Anal Calorim. 2009;96:567–73.
30. Boonchom B, Danvirutai C, Thongkam M. Non-isothermal decomposition kinetics of synthetic serrabrancaite ($MnPO_4{\cdot}H_2O$) precursor in N_2 atmosphere. J Therm Anal Calorim. 2010;99:357–62.
31. Tsao CS, Chen CY, Jeng US, Kuo TY. Precipitation kinetics and transformation of metastable phases in Al–Mg–Si alloys. Acta Mater. 2006;54:4621–31.
32. Moreau G, Cornet JA, Calais D. Accélération de la diffusion chimique sous irradiation dans le système Al-Mg. J Nucl Mater. 1971;38:197–202.
33. Berger D, Cyrener E. Diffusion of foreign elements in aluminum mixed crystals III. Microprobe study of silicon diffusion in aluminum. Neue Huette. 1973;18:356–61.
34. Fujikawa SI, Hirano K, Fukushima Y. Diffusion of silicon in aluminium. Metall Mater Trans A. 1978;9:1811–5.
35. Hirano KI. Diffusion in aluminum. J Jpn Inst Light Met. 1979;29:249–62.
36. Nishizawa T. Thermodynamics of microstructures. ASM Int. 2008.
37. Su T, Jiange H, Gong H. Thermal decomposition and dehydration kinetic studies on hydrated Co(II) methanesulfonate. Thermochim Acta. 2005;435:1–5.
38. Joraid AA. Estimating the activation energy for the non-isothermal crystallization of an amorphous $S_{b9.1}T_{e20.1}S_{e70.8}$ alloy. Thermochim Acta. 2007;456:1–6.
39. Starink MJ. The determination of activation energy from linear heating rate experiments: a comparison of the accuracy of isoconversion methods. Thermochim Acta. 2003;404:163–76.
40. Marioara CD, Andersen SJ, Jansen J, Zandbergen HW. Atomic model for GP-zones in a 6082 Al–Mg–Si System. Acta Mater. 2001;49:321–8.
41. Murayama M, Hono K. Pre-precipitation clusters and precipitation processes in Al–Mg–Si alloys. Acta Mater. 1999;47:1537–48.
42. Ravi C, Wolverton C. First-principles study of crystal structure and stability of Al–Mg–Si–(Cu) precipitates. Acta Mater. 2004;52:4213–27.
43. De Gueser F. Interprétation et traitement des données de sonde atomique tomographique: application à la precipitation dans les Al-Mg-Si. Thesis, Rouen University U.F.R. de Sciences et Techniques, France; 2005.
44. van Huis MA, Chen JH, Zandbergen HW, Sluiter MHF. Phase stability and structural relations of nanometer-sized, matrix-embedded precipitate phase in Al–Mg–Si alloys in the late stage of evolution. Acta Mater. 2006;54:2945–55.
45. Starink MJ, Zahra AM. β' and β precipitation in an Al–Mg alloy studied by DSC and TEM. Acta Mater. 1998;46:3381–97.
46. Ozawa T. Kinetics of non-isothermal crystallization. Polymer. 1971;12:150–8.
47. Liu F, Sommer F, Mittemeijer EJ. Analysis of the kinetics of phase transformations; roles of nucleation index and temperature dependent site saturation, and recipes for the extraction of kinetic parameters. J Mater Sci. 2007;42:573–87.
48. Christian JW. The theory of transformation in metals and alloys, 2nd edn. Part I, chapt. 12. Oxford: Pergamon Press; 1975.
49. Weatherly GC, Nicholson RB. An electron microscope investigation of the interfacial structure of semi-coherent precipitates. Philos Mag. 1968;17:801–31.